Reaction Kinetics, Mechanisms and Catalysis (2021) 134:361–383
https://doi.org/10.1007/s11144-021-02072-y

Immobilization of Mn(II) on Fe_3O_4@Schiff base as an efficient and recoverable magnetic nanocatalyst for the synthesis of hydroquinolines and Hantzsch reaction

Fatemeh Lashkari[1,2] · Rashid Badri[2] · Elham Tahanpesar[2]

Received: 10 June 2021 / Accepted: 8 September 2021 / Published online: 22 September 2021

Abstract

A facile process for the efficient synthesis of a new catalyst is reported by immobilization of Mn(II) on Fe_3O_4@Schiff base. This catalyst is applied for the synthesis of Hantzsch hydroquinoline derivatives. Fourier-transform infrared spectroscopy (FT-IR), X-ray diffraction and transmission electron microscopy analysis were used for the characterization of the as-synthesized catalyst. The products of Hantzsch reaction were characterized using ^{1}H-NMR and FT-IR spectroscopies. Owing to its good magnetic property confirmed by vibrating sample magnetometer analysis, the as-prepared catalyst can be extracted from the reaction mixture easily and apply in the next catalytic cycle. In comparison to the same reactions, this method exhibits the advantages of short reaction times, higher yields, low catalyst loading, easy catalyst separation, catalyst reusability and low cost.

✉ Rashid Badri
rashidbadri@scu.ac.ir; rashidbadri@yahoo.com

[1] Department of Chemistry, Khouzestan Science and Research Branch, Islamic Azad University, Ahvaz, Iran

[2] Department of Chemistry, Ahvaz Branch, Islamic Azad University, Ahvaz, Iran

Graphic abstract

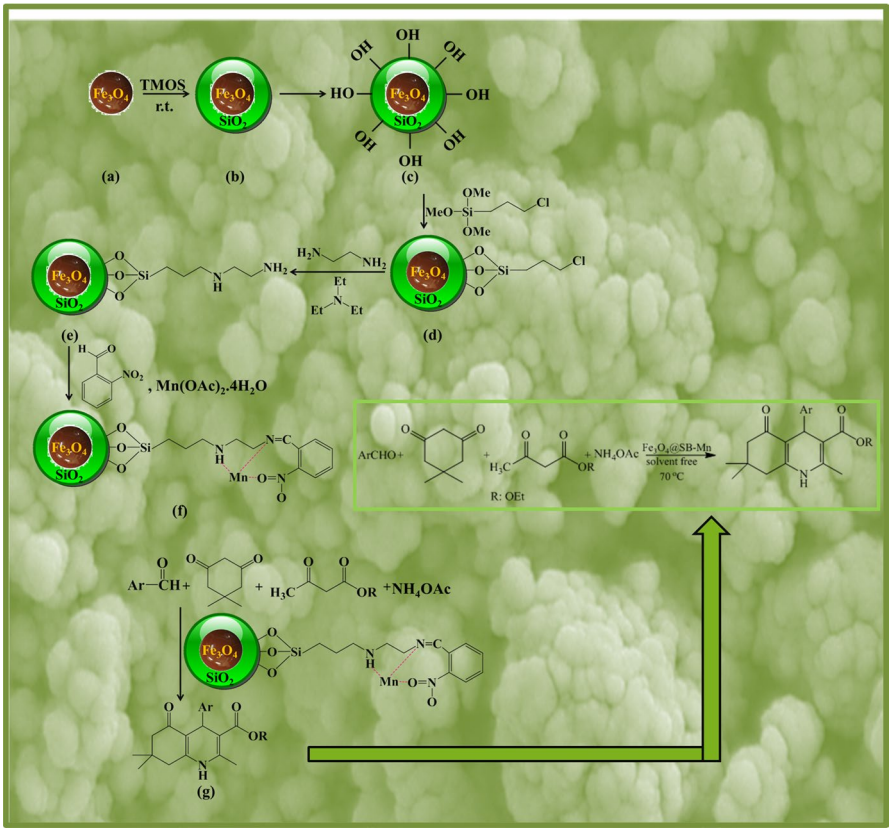

Keywords Hantzsch reaction · Hydroquinoline · Fe_3O_4 nanoparticle · Schiff base

Introduction

Polyhydroquinoline derivatives are one of the main groups of compounds with medical applications and important effect in pharmacological and therapeutic fields, such as hepatoprotective, bronchodilator, antitumor and antidiabetic activities [1, 2]. Furthermore, these compounds can be used for the synthesis of vital drugs such as anti-asthamatics in controlling the Alzheimer's disease or as a chemosensitizer in tumor therapy fields [3]. There are some reports for the synthesis of hydroquinolines, containing condensation of aldehydes with ethyl acetoacetate in the presence of ammonia and acetic acid by refluxing for a long time [4]. Long reaction times, low product yields and harsh reaction conditions are some of the disadvantages of the reported methods [2]. To solve these problems, some alternate strategies have been developed using ionic liquids [5], solar thermal energy [6], HY-Zeolite

[7], cerium(IV) ammonium nitrate [8], nickel nanoparticles [9] and irradiations of microwave or ultrasound [10, 11]. Despite the advantages of each of these applied methods, using environmentally harmful or expensive catalysts, harsh reaction conditions such as high temperatures remain the challenges of these strategies. In addition to the above challenges that limit this kind of reactions, another problem is the stability, recoverability and reusability of the catalysts during the work-up process [2] that we try to improve. Nanocatalysts with high surface-to-volume ratios and larger number of active sites on the surfaces exhibit a great potential for progressing the reactions in comparison to the bulk catalysts [12]. Magnetic nanocatalysts such as Fe_3O_4 have attracted considerable interest in the field of heterogeneous catalysis due to their easy separation from the reaction medium and recoverability [13]. Having low cost and being comparatively non-toxic are the other advantages of these paramagnetic catalysts [14]. These benefits make Fe_3O_4-based nanocatalysts interesting for applying as heterogeneous catalysts in various reactions such as C–C coupling reaction of Suzuki–Miyaura [15] and Sonogashira [16] or synthesis of propargylic amines [17], 3-[(2-chloroquinolin-3-yl)methyl]pyrimidin-4(3H)ones [18], quinoxalines [19], etc. In order to improve the stability of catalysts during the reaction processes and work-up, immobilization of metals on the magnetic supports can be an effective strategy. Also there are some reports on using magnetism for stabilizing the crystal structure of metals [20]. Finding a stable and easy recoverable catalyst that progress the reaction process in a milder reaction conditions with higher yields is our aim in this investigation. Fe_3O_4-based nanocatalysts can provide the advantages such as easy extraction and recovery using an external magnet instead of filtration and centrifugation, being environmentally friendly, low cost and simplicity in synthesis, having non-corrosive nature, being moisture insensitive that make them ideal heterogeneous catalysts for Hantzsch reaction and hydroquinoline derivatives formation.

Experimental

Materials and methods

Chemical precursors and solvents were purchased from Sigma-Aldrich company. X-ray diffraction (XRD) analysis was done using a Bruker AXS (D8 Advance) instrument applying the reflection Bragg–Brentano geometry with Cu K_α radiation ($\lambda = 1.5406$ Å). Transmission electron microscopy (TEM) was applied to investigate the morphology and size of the as-synthesized or recycled catalyst using a Philips, CM-10 TEM instrument operated at 100 kV. Fourier-transform infrared (FT-IR) spectra were obtained using a FT-IR JASCO-8600 spectrometer, Japan. To obtain melting point data, a Barnstead Electrothermal (BI 9300) apparatus was applied. NMR spectra were recorded using a Bruker spectrometer (400 MHz) using DMSO-d_6 solvent. Field-emission scanning electron microscopy (FE-SEM) and energy dispersive analysis of X-ray (EDAX) analysis were obtained using Philips XL30 instrument, accelerating voltage of 20 kV, to distinguish the morphology and elemental composition of the as synthesized catalyst. LBKFB, Iran was used to investigate the

magnetic behavior of the catalyst applying vibrating sample magnetometer (VSM) analysis. To investigate the thermal behavior of the nanocatalyst, thermal gravimetric analysis (TGA) was used (Simultaneous Thermal Analyzer, STA 6000, Perkin Elmer, USA, conditions: 30 mg nanocatalyst, the heating rate of 10 °C min^{-1}, using the atmosphere of nitrogen and oxygen). Ninhydrin test of Fe_3O_4@SiO_2-pr-NH-CH_2-CH_2-NH_2 was done to detect free NH_2 groups.

Fe_3O_4 nanoparticles synthesis

Magnetic nanoparticles of Fe_3O_4 were synthesized according to the modified reported procedure [13]. In brief, $FeCl_2{\cdot}4H_2O$ (2 g) and $FeCl_3{\cdot}6H_2O$ (3 g) were poured to the round bottom flask that contains concentrated hydrochloric acid (25 mL) and sonicated to obtain a homogeneous solution. In the next step, ammonia solution (40 mL, 25%) was added dropwisely under argon atmosphere. The obtained solution was refluxed for 0.5 h under magnetic stirring. After that, the mixture was filtered and washed with distilled water several times and dried in 60 °C oven for 12 h. The obtained dark powder was Fe_3O_4 magnetic nanoparticles.

Synthesis of magnetic Fe_3O_4 nanoparticles coated by silica (Fe_3O_4@SiO_2 nanostructures)

Fe_3O_4 nanoparticles obtained from previous section (1 g) were added to the reaction flask charged by distilled water (50 mL) and ethanol (150 mL) and sonicated for 30 min at room temperature. Ammonia solution (3.5 mL, 25% W), was added. After 10 min stirring, tetramethoxysilane (TMOS, 0.7 mmol) was added dropwisely and stirred for 16 h at room temperature. The product was removed from the solution using an external magnet and washed with distilled water and ethanol several times. The product was dried in 60 °C oven for 6 h which was Fe_3O_4@SiO_2.

Magnetic Fe_3O_4 nanoparticles modified by Schiff Base (Fe_3O_4@SB nanostructures)

For the synthesis of Fe_3O_4@SB nanostructures, Fe_3O_4@SiO_2 from the previous Sect. (1 g) was added to the three-necked round bottom flask charged by dry toluene and sonicated for 30 min. (3-chloropropyl)triethoxysilane (0.8 mmol) was added to the reaction mixture and refluxed for 24 h under argon atmosphere. The product was removed from the reaction mixture by external magnet, washed by ethanol followed by drying in 60 °C oven for 5 h. The obtained product was Fe_3O_4@SiO_2-prCl in this step. In the second step, Fe_3O_4@SiO_2-prCl (1 g) was dispersed in dry toluene (50 mL) by ultrasonic irradiation for 30 min. Then ethylenediamine (5 mmol) and triethylamine (0.015 mmol) was added and refluxed for 24 h using argon. The product was removed using a magnet followed by washing with ethanol. At last, the product was dried in 50 °C oven for 4 h. This product was Fe_3O_4@SiO_2-pr-NH-CH_2-CH_2-NH_2. In the last step, the previous product (1 g) was dispersed in dry toluene (40 mL) using ultrasonic bath for 50 min followed by the addition of 2-nitrobenzaldehyde (4 mmol), refluxed for 24 h under

argon atmosphere and extracted from the reaction mixture using a magnet like previous steps. The obtained precipitate was washed with ethanol several times and dried at 50 °C to obtain Fe_3O_4@SB nanostructures.

Immobilization of Mn(II) on Fe_3O_4@SB (Fe_3O_4@SB-Mn(II))

For this immobilization, Fe_3O_4@SB (1.1 g) was dispersed in ethanol (15 mL) at room temperature. A reaction flask was charged by ethanolic solution of $Mn(OAc)_2{\cdot}4H_2O$ (0.688 g, 15 mL) and stirred for 30 min. Both solutions were added to the round bottom flask (100 mL) and refluxed for 24 h at 60 °C. The solid brown product was washed by ethanol (150 mL) and distilled water (100 mL) and extracted using a magnet. The obtained Fe_3O_4@SB-Mn was dried in 70 °C oven for 6 h. The product structure is illustrated in Fig. 1.

Investigating the catalytic activity and general method for the synthesis of polyhydroquinoline using Fe_3O_4@SB-Mn

The Hantzsch pyridine synthesis or Hantzsch 1,4-dihydropyridine synthesis is a one-step reaction in the presence of benzaldehyde, ethyl acetoacetate, dimedone and ammonium acetate. To do this, benzaldehyde (1 mmol), ethyl acetoacetate (1 mmol), dimedone (1 mmol) and ammonium acetate (1.5 mmol) in the presence of Fe_3O_4@SB-Mn (0.002 g) as a catalyst were added to the reaction flask at 70 °C and stirred. The reaction progress was monitored using thin layer chromatography (TLC). After the reaction completion, hot ethanol was added to the reaction mixture followed by extracting the catalyst using an external magnet. Cubes of ice was added, the produced precipitate was extracted and recrystallized in ethanol.

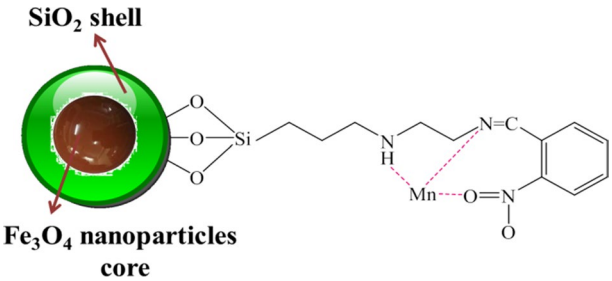

Fig. 1 Schematic illustration for immobilization of Mn(II) on Fe_3O_4@SB at 60 °C using ethanolic solution of Fe_3O_4@SB and $Mn(OAc)_2{\cdot}4H_2O$ with the following synthetic steps: (i) dispersing the Fe_3O_4@SB in ethanol, (ii) dispersing the $Mn(OAc)_2{\cdot}4H_2O$ in ethanol, (iii) addition of these two solutions to the reaction flask followed by refluxing at 60 °C, (iv) washing the brown product using ethanol and water and (v) drying at 70 °C for 6 h to obtain a Mn(II) on Fe_3O_4@SB product

Fig. 2 Catalyst formation steps; **a** Fe_3O_4 nanoparticles synthesis applying $FeCl_2{\cdot}4H_2O$ and $FeCl_3{\cdot}6H_2O$, ▶ HCl, ammonia solution under reflux and argon atmosphere, drying at 60 °C for 12 h, **b** Fe_3O_4 nanoparticles coated by silica using dispersed Fe_3O_4 nanoparticles in the distilled water and ethanol mixture in the presence of ammonia solution and tetramethoxysilane following by 16 h stirring at room temperature, washing by water and ethanol and drying in 60 °C for 6 h, **c** Fe_3O_4 nanoparticles coated by silica solvated in the reaction medium of ethanol and water, **d** formation of Fe_3O_4@SiO_2-prCl using Fe_3O_4@SiO_2 dispersed in dry toluene following by the addition of (3-chloropropyl)triethoxysilane and refluxing for 24 h under argon atmosphere, washing with ethanol and drying at 60 °C for 5 h, **e** Fe_3O_4@SiO_2-pr-NH–CH_2–CH_2–NH_2 formation using Fe_3O_4@SiO_2-prCl dispersed in dry toluene following by the addition of ethylenediamine and triethylamine and refluxing for 24 h under argon atmosphere, washing with ethanol and drying in 50 °C for 4 h, **f** immobilization of Mn(II) on Fe_3O_4@SB by the dispersion of Fe_3O_4@SiO_2-pr-NH–CH_2–CH_2–NH_2 in dry toluene following by the addition of 2-nitrobenzaldehyde, refluxing for 24 h under argon atmosphere, washing with ethanol and drying at 50 °C, **g** Hantzsch reaction in the presence of benzaldehyde, ethyl acetoacetate, dimedone, ammonium acetate and Fe_3O_4@SB-Mn(II) nanocatalyst at 70 °C

Recyclability and reusability of Fe_3O_4@SB-Mn catalyst

A flask was charged by benzaldehyde (1 mmol), ethyl acetoacetate (1 mmol), dimedone (1 mmol), ammonium acetate (1.5 mmol) and catalyst (0.002 g) and stirred at 70 °C up to TLC test confirm the reaction completion. Hot ethanol was added and the catalyst was removed from the reaction mixture, washed and dried. Then used in another cycle of catalytic reaction. This catalyst can progress the reaction for 9 cycles without a considerable decrease in yield or leaching.

Results and discussion

Immobilization of Mn(II) on the surface of Fe_3O_4@SB was applied successfully. Fig. 2 shows the details of each step. This catalyst exhibited interesting catalytic activity in progressing Hantzsch reaction (Fig. 2g).

Each step was characterized using FT-IR analysis. In the case of Fe_3O_4 nanoparticles (Fig. 3a), two characteristic bands at 577 cm^{-1} (Fe–O) and 3410 cm^{-1} (stretching vibration of O–H) were observed [21]. Fig. 3b shows the FT-IR spectrum of Fe_3O_4@SiO_2 nanostructures with symmetric and asymmetric vibrations of ν_s(O–Si–O, 928 cm^{-1}) and ν_{as}(O–Si–O, 1105 cm^{-1}) [22]. Fig. 3c belongs to Fe_3O_4@SiO_2-prCl nanostructures. The stretching vibration of (–CH_2–) appears at 2853 cm^{-1}. Also, the stretching vibration of (–Si–O–) linked to the (-CH_2) is at 1100 cm^{-1} that covers with ν_{as}(O–Si–O, 1105 cm^{-1}) [21]. N–H bending (2800 cm^{-1}) and –OH and –NH stretching (3200–3400 cm^{-1}) confirm the formation of Fe_3O_4@SiO_2-pr-NH–CH_2–CH_2–NH_2 (Fig. 3d). Fe_3O_4@SB nanostructures confirm the presence of C=N (1300 cm^{-1}) and aromatic C–H (3100 cm^{-1}) (Fig. 3e). Fig. 3f confirms the formation of Fe_3O_4@SB-Mn(II) nanocatalyst.

XRD analysis was used to characterize the Fe_3O_4@SB-Mn(II) nanocatalysts. Fig. 4a shows the theoretical XRD pattern for Fe_3O_4 nanoparticles using VESTA software. Fig. 4b shows the experimental data of Fe_3O_4@SB-Mn(II) nanocatalysts. Bragg reflections by ([220], [311], [222], [400], [110], [422], [511], [440],

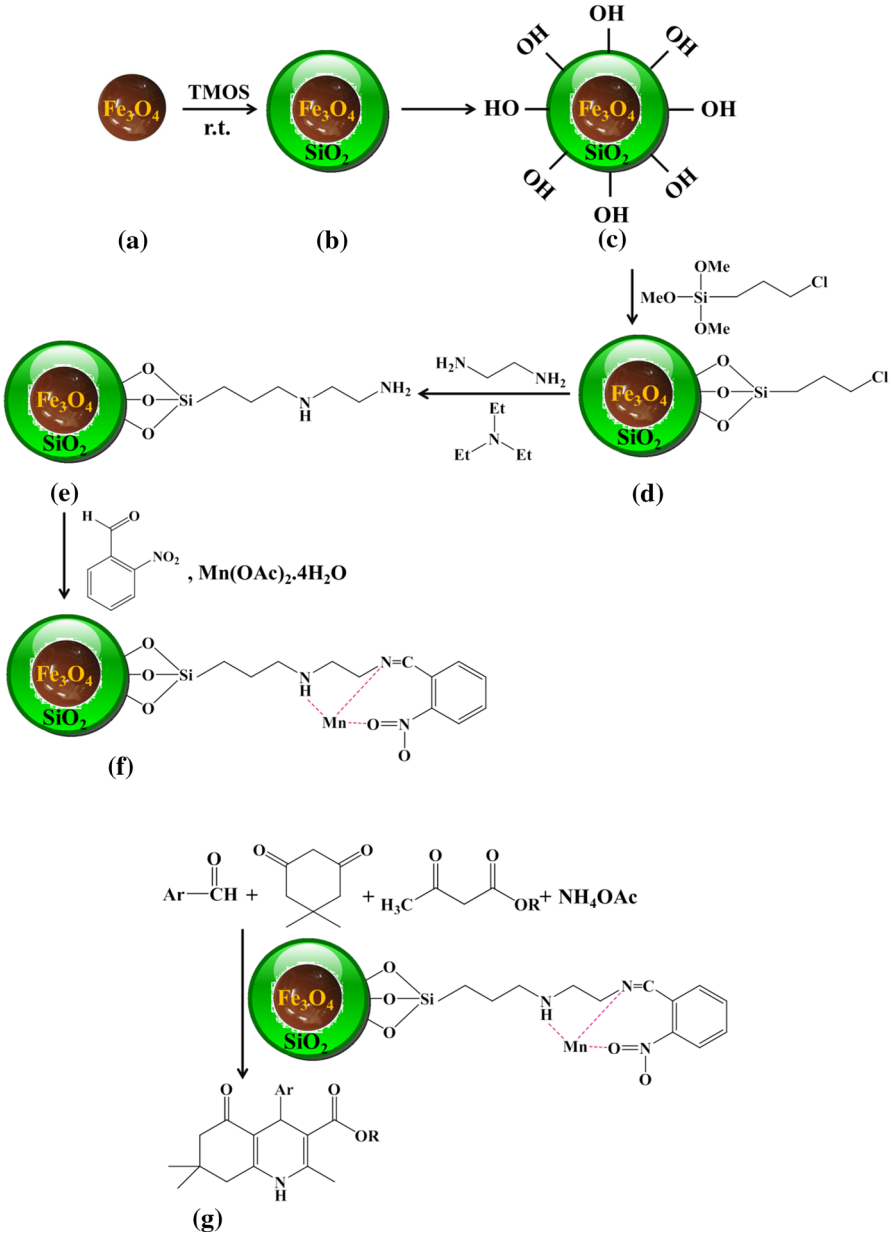

[620] and [533]) indices at 2θ = 30°, 35°, 37°, 43°, 46°, 53°, 57°, 63°, 71° and 75° confirm the presence of Fe_3O_4 nanoparticles in the catalyst structure [13]. Comparing Fig. 4b with 4a exhibits that the peaks are shifted to higher 2θ values (2° shift) which confirms the product formation.

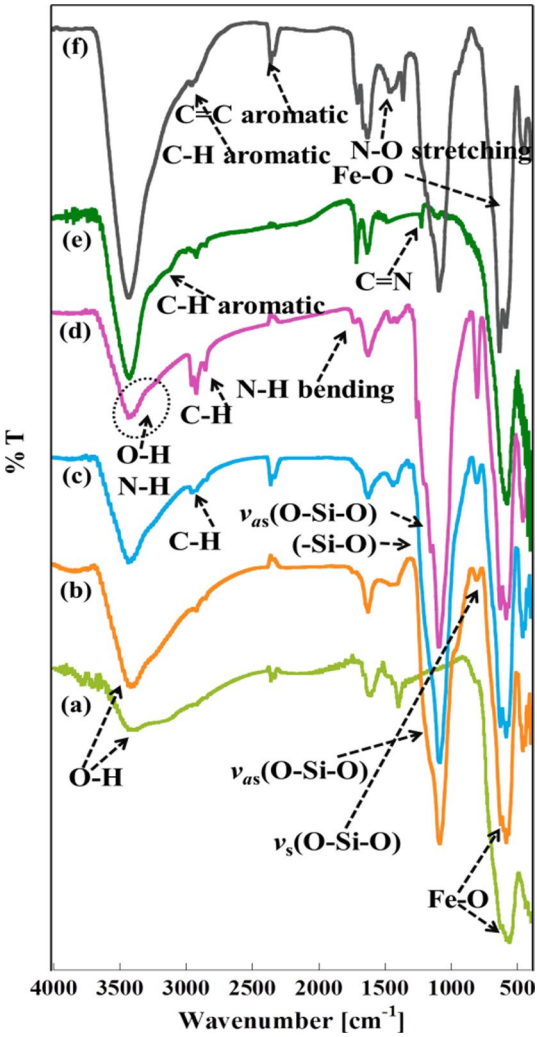

Fig. 3 FT-IR spectra of *a* Fe_3O_4 nanoparticles, *b* Fe_3O_4@SiO_2 nanostructures, *c* Fe_3O_4@SiO_2-prCl nanostructures, *d* Fe_3O_4@SiO_2-pr-NH–CH_2–CH_2–NH_2, *e* Fe_3O_4@SB nanostructures and *f* Fe_3O_4@SB-Mn(II) nanocatalyst using a dry KBr (spectroscopic grade dried in 110 °C oven, 24 h) for the formation of pellets

FE-SEM analysis was performed to examine the morphology of the as-prepared catalyst. Spherical nanostructures were observed (Fig. 5).

EDAX analysis was applied for elemental characterization of the as-prepared catalyst that confirms the presence of C, N, Fe, Mn, O and Si elements in the prepared structure (Fig. 6).

TEM analysis was applied to investigate the morphology and size of the as-prepared Fe_3O_4@SB-Mn(II) nanocatalyst. Mn nanoparticles with the mean diameter of 5 nm are obvious on the Fe_3O_4@SB support (Fig. 7).

To investigate the weight change amount of a catalyst as a function of increasing temperature, thermogravimetric analysis (TGA) was applied in an atmosphere of nitrogen and oxygen (Fig. 8). In this measurement, the mass variation is measured

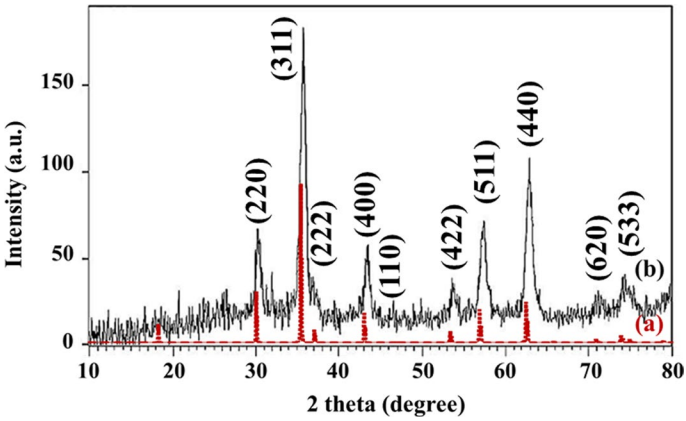

Fig. 4 XRD patterns of *a* theoretical Fe_3O_4 using VESTA software and *b* the as-synthesized Fe_3O_4@SB-Mn(II) nanocatalyst using a powder sample

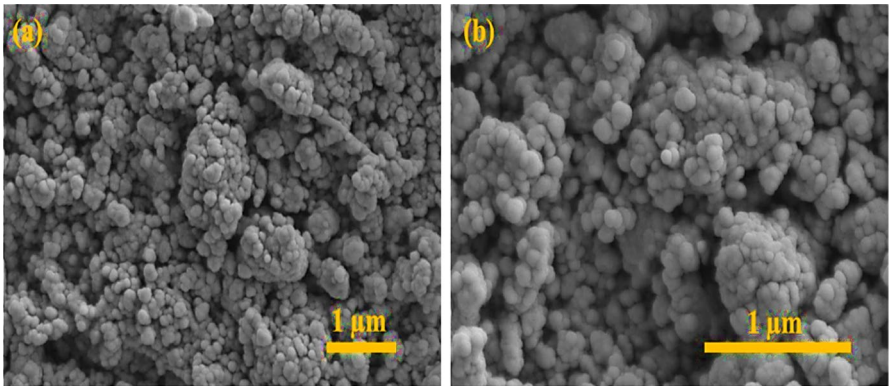

Fig. 5 **a**, **b** FE-SEM images of the as-synthesized Fe_3O_4@SB-Mn(II) nanocatalyst using a small portion of the catalyst dispersed in ethanol and transferring to the aluminum stub of the FE-SEM instrument and air-drying

over time when the temperature is elevated up to 800 °C. The weight change of a catalyst was occurred in two steps, (i) water and alcoholic solutions were removed up to 200 °C and (ii) organic functional groups of Schiff base were removed up to 550 °C. Furthermore, this analysis confirms the thermal stability of silica shell around the magnetic Fe_3O_4 nanoparticles.

Vibrating sample magnetometer (VSM) measurement was applied to investigate the magnetic behavior of Fe_3O_4@SB-Mn(II) nanocatalyst (Fig. 9). This room temperature analysis leads to obtain a magnetization curve which is a function of the applied field. No hysteresis loop was found in the case of this catalyst. In comparison to pure Fe_3O_4 nanoparticles, the saturation magnetization value is decreased from 60 to about 17 emu/g which is mainly due to the presence of nonmagnetic SiO_2 and SB groups on the surface of Fe_3O_4@SB-Mn(II) nanocatalyst [23, 24].

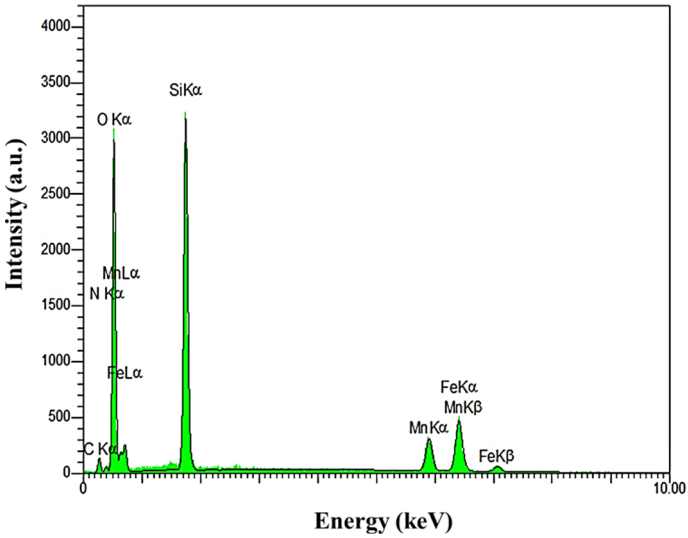

Fig. 6 EDAX analysis of Fe_3O_4@SB-Mn(II) nanocatalyst using a small portion of the catalyst dispersed in ethanol and transferring to the aluminum stub of the FE-SEM instrument and air-drying

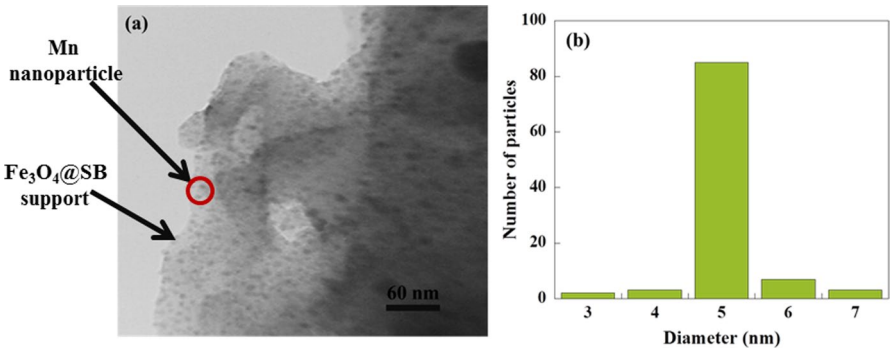

Fig. 7 **a** TEM image and **b** histogram of particles size distribution for the as-synthesized Fe_3O_4@SB-Mn(II) nanocatalyst by dispersing a small portion of the catalyst in the ethanol and transferring it to the copper grid of the TEM instrument

In order to detect free NH_2 groups, ninhydrin color test [25, 26] of Fe_3O_4@SiO_2-pr-NH–CH_2–CH_2–NH_2 was done by heating the as-prepared structure in 2% ethanol solution of ninhydrin followed by violet color formation which confirms the presence of amine groups in the Fe_3O_4@SiO_2-pr-NH–CH_2–CH_2–NH_2 structure.

As mentioned above, this catalyst was applied in Hantzsch reaction using benzaldehyde, ethyl acetoacetate, dimedone and ammonium acetate. Table 1 shows the condition optimization and Table 2 shows the details.

According to Table 1, solvent free condition at 70 °C and in the presence of 0.002 g catalyst was the best condition. The catalytic activity of Fe_3O_4@SB-Mn(II)

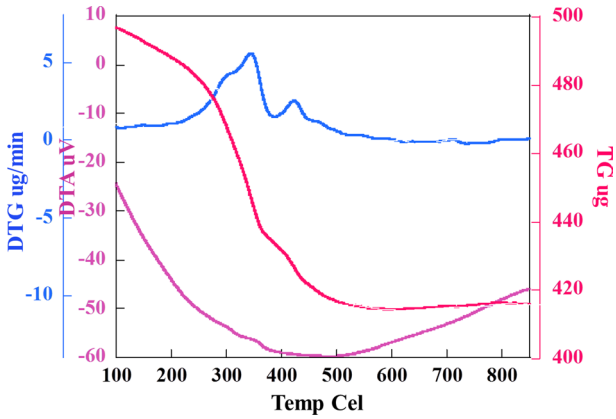

Fig. 8 TGA analysis, derivative thermal gravimetric (DTG) and differential thermal analysis (DTA) curves of the as-synthesized Fe_3O_4@SB-Mn(II) nanocatalyst applied in an atmosphere of nitrogen and oxygen and temperature range of 100–800 °C

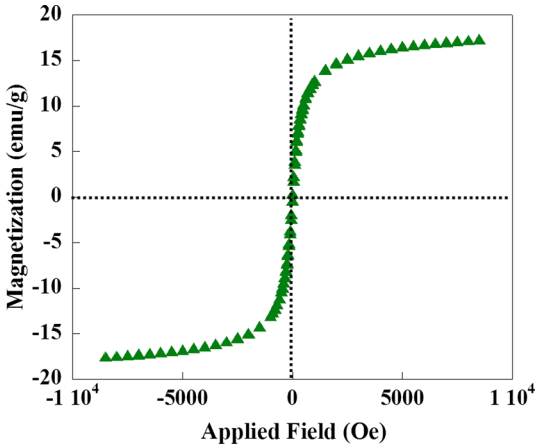

Fig. 9 VSM curve of the as-synthesized Fe_3O_4@SB-Mn(II) nanocatalyst at room temperature with no hysteresis loop

nanocatalyst is compared with other reported catalysts in similar conditions in Table 3. The extracted catalyst was washed and dried for applying in nine catalytic cycles with no considerable loss in catalytic activity or products yield (Fig. 10). Also, TEM analysis was applied after the reusability tests (Fig. 11) which shows no considerable agglomeration in the structure. Furthermore, the details of the proposed mechanism are illustrated in the presence of Fe_3O_4@SB-Mn catalyst (Fig. 12). The details of the products synthesis are exhibited in the NMR and FT-IR data section.

NMR and FT-IR data

(1a): Ethyl 2,7,7-trimethyl-5-oxo-4-phenyl-1,4,6,6,8,8-hexahydroquinoline-3-carboxylate [29]. M.P.: 225–232 °C; IR (KBr, cm^{-1}): 3288 (NH stretching), 3079

Table 1 Optimizing the reaction conditions (solvent, temperature and time) in Hantzsch reaction using Fe_3O_4@SB-Mn(II) nanocatalyst in the presence of benzaldehyde (1 mmol), ethyl acetoacetate (1 mmol), dimedone (1 mmol) and ammonium acetate (1.5 mmol)

Entry	Catalyst amount (mg)	Solvent	Temperature (°C)	Time (min)	Yield (%)
1	2	Toluene	70	20	25
2	2	Water	70	20	50
3	2	Solvent free	70	20	92
4	2	Ethanol	70	20	80
5	2	Solvent free	R. T	20	25
6	2	Solvent free	40	20	45
7	2	Solvent free	85	20	92
8	5	Solvent free	70	20	92
9	1	Solvent free	70	20	85
10	0.5	Solvent free	70	20	62

(=C–H stretching vibration, sp^2), 2960 (C–H stretching vibration, sp^3), 1698 (C=O ester), 1608 (C=O ketone), 1486 (C=C, Ar), 1213 (C–O, ester). Mass (m/z): 339 (M), 324 ($C_{20}H_{22}NO_3$), 262.2 ($C_{13}H_{16}NO_3$), 234 ($C_{13}H_{16}NO_3$).

(1b): Ethyl 2,7,7-trimethyl-5-oxo-4-(4-methoxy-phenyl)-1,4,6,6,8,8-hexahydroquinoline-3-carboxylate [30]. M. P.: 257–259 °C; IR (KBr, cm^{-1}): 3278 (NH stretching), 3208 3077, 2987 (C–H stretching vibration, sp^3), 1701 (C=O ester), 1649 (C=O ketone), 1494 (C=C, Ar), 1214 (C–O, ester). Mass (m/z): 369.2 (M), 340.2 ($C_{20}H_{22}NO_4$), 324.2 ($C_{20}H_{22}NO_3$), 296.2 ($C_{19}H_{22}NO_2$), 234.1 ($C_{13}H_{16}NO_3$), 252.2 ($C_{17}H_{18}NO$).

(1c): Ethyl 2,7,7-trimethyl-5-oxo-4-(*p*-tolyl)-1,4,6,6,8,8-hexahydroquinoline-3-carboxylate [29]. M. P.: 261–263 °C; IR (KBr, cm^{-1}): 3207 (NH stretching), 3077 (=C–H stretching vibration, sp^2), 2958 (C–H stretching vibration, sp^3), 1700 (C=O ester), 1648 (C=O ketone), 1494 (C=C, Ar), 1214 (C–O, ester).

(1d): Ethyl-4-(4-chlorophenyl)-2,7,7-trimethyl-5-oxo-1,4,6,6,8,8-hexahydroquinoline-3-carboxylate [30]. M. P.: 244–246 °C; IR (KBr, cm^{-1}): 3207 (NH stretching), 3077 (=C–H stretching vibration, sp^2), 2958 (C–H stretching vibration, sp^3), 1700 (C=O ester), 1646 (C=O ketone), 1486 (C=C, Ar), 1214 (C–O, ester), 850 (Ar–Cl)*para*.

(1e): Ethyl 2,7,7-trimethyl-4-(4-nitrophenyl)-5-oxo-1,4,6,6,8,8-hexahydroquinoline-3-carboxylate [30]. M. P.: 241–243 °C; IR (KBr, cm^{-1}): 3274 (NH stretching), 3075 (=C–H stretching vibration, sp^2), 2965 (C–H stretching vibration, sp^3), 1702 (C=O ester), 1648 (C=O ketone), 1494 (C=C, Ar), 1519 (Ar-NO_2) *para*, 1216 (C–O, ester), 831 (C–N). Mass (m/z): 384 (M), 369.2 ($C_{19}H_{20}N_2O_5$), 262.2 ($C_{15}H_{20}NO_3$).

(1f): Ethyl 4-(2-chlorophenyl)-2,7,7-trimethyl-5-oxo-1,4,6,6,8,8,-hexahydroquinoline-3-carboxylate [31]. M. P.: 206–208 °C; IR (KBr, cm^{-1}): 3291 (NH stretching), 3074 (=C–H stretching vibration, sp^2), 2958 (C–H stretching vibration, sp^3), 1697 (C=O ester), 1639 (C=O ketone), 1486 (C=C, Ar), 1213 (C–O, ester), 790 (Ar–Cl) *ortho*.

Table 2 Hantzsch reaction and formation of 1,4-dihydropyridines in the presence of Fe_3O_4@SB-Mn(II) nanocatalyst under optimum conditions (benzaldehyde (1 mmol), ethyl acetoacetate (1 mmol), dimedone (1 mmol) and ammonium acetate (1.5 mmol) and solvent free condition at 70 °C)

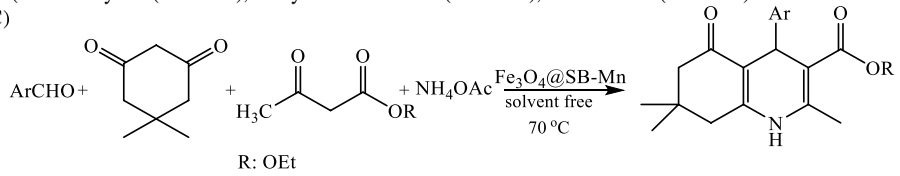

Entry	Aldehyde	R_2	Product	Time (min)	Yield %	M. P. (°C) (found)	M. P. (°C) (reported)
1	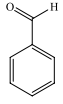	OEt	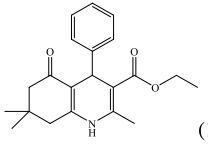 (1a)	15	92	225–232	224–226
2	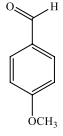	OEt	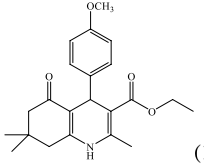 (1b)	35	95	257–259	257–259
3	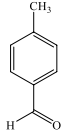	OEt	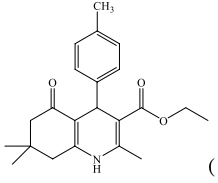 (1c)	30	95	261–263	259–262

Table 2 (continued)

Entry	Aldehyde	R_2	Product	Time (min)	Yield %	M. P. (°C) (found)	M. P. (°C) (reported)
4	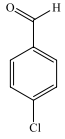	OEt	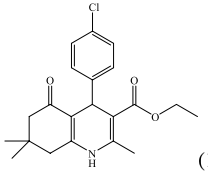 (1d)	15	90	244–246	244–246
5	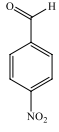	OEt	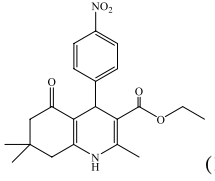 (1e)	10	98	241–243	242–244
6	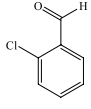	OEt	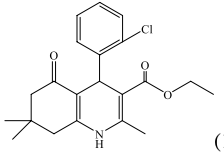 (1f)	25	92	206–208	207–209
7	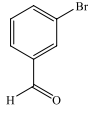	OEt	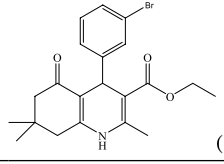 (1 g)	25	95	234–236	235–236

Table 2 (continued)

Entry	Aldehyde	R_2	Product	Time (min)	Yield %	M. P. (°C) (found)	M. P. (°C) (reported)
8	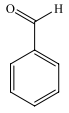	OMe	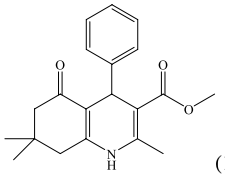 (1 h)	20	92	259–260	260–262
9	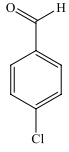	OMe	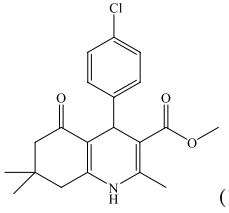 (1i)	15	93	220–222	219–222
10	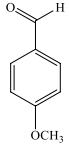	OMe	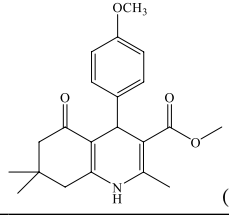 (1j)	35	96	258–259	257–259

Table 2 (continued)

Entry	Aldehyde	R_2	Product	Time (min)	Yield %	M. P. (°C) (found)	M. P. (°C) (reported)
11	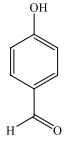	OMe	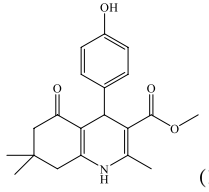 (1 k)	35	93	299–301	–
12	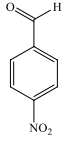	OMe	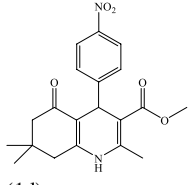 (1 l)	10	95	241–243	–
13	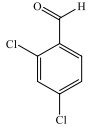	OEt	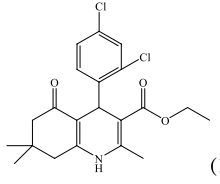 (1d)	30	90	211–213	–
14	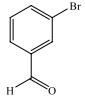	OMe	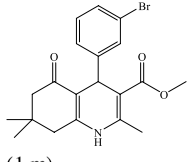 (1 m)	25	95	234–236	233–234

Table 3 Comparing the obtained data with other similar reactions in the presence of different catalysts

Entry	R_1	R_2	Catalyst	Time (min)	Solvent	Temperature (°C)	Yield (%)	References
1		OEt	MgO nanoparticles[a]	90	Ethanol	Reflux	88	[27]
2	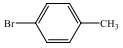	OEt	MgO nanoparticles[a]	95	Ethanol	Reflux	90	[27]
3	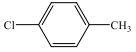	OEt	MgO nanoparticles[a]	80	Ethanol	Reflux	94	[27]
4	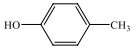	OEt	MgO nanoparticles[a]	50	Ethanol	Reflux	95	[27]
5	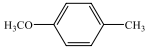	OEt	MgO nanoparticles[a]	55	Ethanol	Reflux	96	[27]
6		OEt	MgO nanoparticles[a]	50	Ethanol	Reflux	98	[27]
7		OEt	MgO nanoparticles[a]	55	Ethanol	Reflux	80	[27]
8	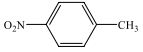	OEt	MgO nanoparticles[a]	100	Ethanol	Reflux	75	[27]
9		OEt	Catalyst-free[b]	10	Solvent-free	100	73	[28]
10		OEt	Catalyst-free[b]	10	Solvent-free	100	98	[28]
11		OEt	Catalyst-free[b]	10	Solvent-free	100	92	[28]

Table 3 (continued)

Entry	R_1	R_2	Catalyst	Time (min)	Solvent	Temperature (°C)	Yield (%)	References
12		OEt	Catalyst-free[b]	10	Solvent-free	100	99	[28]
13		OEt	Catalyst-free[b]	5	Solvent-free	100	91	[28]
14	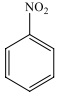	OEt	Fe_3O_4@SB-Mn	10	Solvent-free	70	98	This work
15	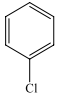	OEt	Fe_3O_4@SB-Mn	15	Solvent-free	70	90	This work
16		OEt	Fe_3O_4@SB-Mn	15	Solvent-free	70	92	This work

[a] 1 mmol aryl aldehyde, 1 mmol ethyl acetoacetate, 1 mmol ammonium acetate, 1 mmol dimedone, 0.03 g catalyst

[b] 1 mmol aryl aldehyde, 2 mmol dimedone, 1 mmol ethyl acetoacetate, 1.5 mmol ammonium acetate

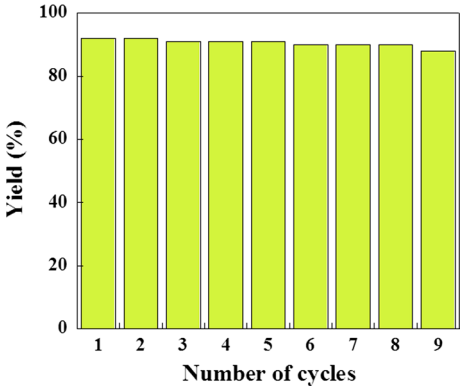

Fig. 10 Reusability of Fe_3O_4@SB-Mn catalyst in Hantzsch reaction and formation of 1,4-dihydropyridines which take place between benzaldehyde (1 mmol), ethyl acetoacetate (1 mmol), dimedone (1 mmol) and ammonium acetate (1.5 mmol) using hot ethanol to extract the catalyst from the reaction mixture followed by washing and drying. Then used in another cycle of catalytic reaction which progress the reaction for nine cycles without a considerable decrease in yield or leaching

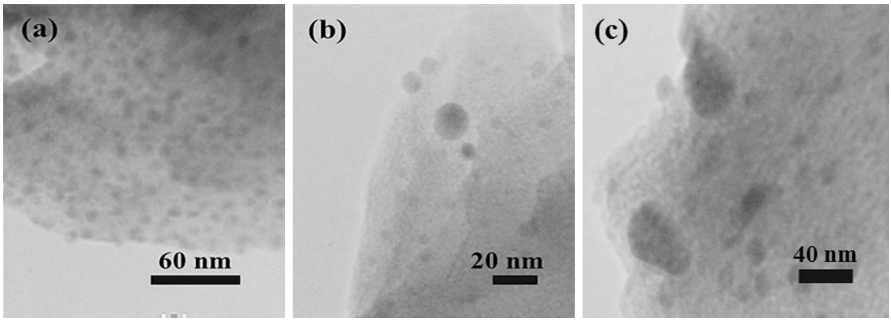

Fig. 11 **a–c** TEM analysis for the Fe_3O_4@SB-Mn(II) nanocatalyst after the reusability test

(1g): Ethyl 4-(3-bromophenyl)-2,7,7-trimethyl-5-oxo-1,4,6,6,8,8-hexahydroquinoline-3-carboxylate [29]. M. P.: 234–236 °C; IR (KBr, cm^{-1}): 3207 (NH stretching), 3073 (=C–H stretching vibration, sp^2), 2956 (C–H stretching vibration, sp^3), 1702 (C=O ester), 1643 (C=O ketone), 1490 (C=C, Ar), 1211 (C–O, ester), 543 (Ar–Br) *meta*.

(1h): Methyl 2,7,7-trimethyl-5-oxo-4-phenyl-1,4,6,6,8,8-hexahydroquinoline-3-carboxylate [31]. M. P.: 259–260 °C; IR (KBr, cm^{-1}): 3303 (NH stretching), 3072 (=C–H stretching vibration, sp^2), 2977 (C–H stretching vibration, sp^3), 1685 (C=O ester), 1648 (C=O ketone), 1511 (C=C, Ar), 1226 (C–O, ester).

(1i) [29]**:** M. P.: 220–222 °C; IR (KBr, cm^{-1}): 3187 (NH stretching), 3070 (=C–H stretching vibration, sp^2), 2958 (C–H stretching vibration, sp^3), 1708 (C=O ester), 1606 (C=O ketone), 1490 (C=C, Ar), 1218 (C–O, ester), 842 (Ar–Cl) *para*.

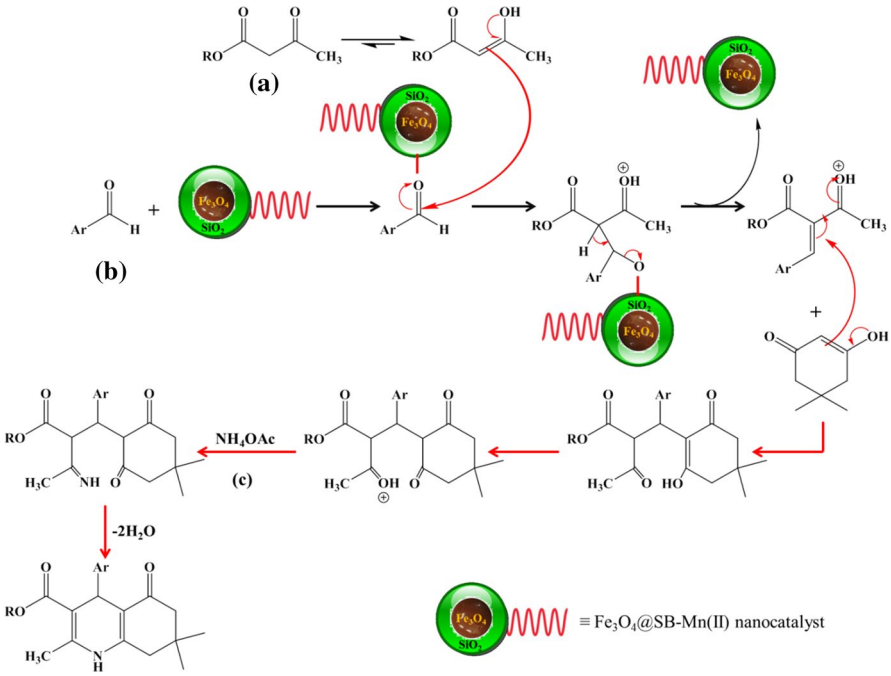

Fig. 12 Details of the proposed mechanism in Hantzsch reaction and formation of 1,4-dihydropyridines in the presence of Fe_3O_4@SB-Mn catalyst

(1j): Methyl 4-(4-methoxyphenyl)-2,7,7-trimethyl-5-oxo-1,4,6,6,8,8-hexahydroquinoline-3-carboxylate [29]. M. P.: 258–259 °C; IR (KBr, cm^{-1}): 3274 (NH stretching), 3070, 2987 (C–H stretching vibration, sp^3), 1701 (C = O ester), 1649 (C = O ketone), 1496 (C = C, Ar), 1214 (C–O, ester).

1(k): Methyl 4-(4-hydroxyphenyl)-2,7,7-trimethyl-5-oxo-1,4,6,6,8,8-hexahydroquinoline-3-carboxylate M.P.: 299–301 °C; IR (KBr, cm^{-1}): 3429, 3222 (NH, OH stretching), 2995 (C–H stretching vibration, sp^3), 1705 (C = O ester), 1655 (C = O ketone), 1490 (C = C, Ar), 1220 (C–O, ester). ^{1}H-NMR (400 MHz, DMSO-d_6): δ (ppm) 0.8 (s, 3Ha), 1.05 (s, 3Ha'), 1.98 (d, J = 16.0 Hz, 3Hb), 2.12 (d, J = 20.0 Hz, 1Hb'), 2.27 (d, J = 16.0 Hz, 1Hc), 2.28 (s, 3Hd), 2.40 (d, J = 16.0 Hz, 1Hc'), 3.53 (s, 3He), 4.76 (s, 1Hf), 6.57 (d, J = 12.0 Hz, 1Hg), 6.92 (d, J = 10.0 Hz, 1Hh), 9.01 (s, NH), 9.06 (s, OH). ^{13}C-NMR (400 MHz, DMSO-d_6) δ (ppm) 18.7, 26.9, 29.6, 31.1, 32.6, 35.0, 39.3, 40.6, 104.1, 110.8, 115.0, 128.6, 138.7, 145.2, 149.5, 155.7, 167.9, 194.8. Mass (m/z): 341.2 (M), 239.1 ($C_{16}H_{17}NO$).

(1 l): Methyl 2,7,7-trimethyl-4-(4-nitrophenyl)-5-oxo-1,4,6,6,8,8-hexahydroquinoline-3-carboxylate M. P.: 241–243 °C; IR (KBr, cm^{-1}): 3191 (NH stretching), 3073 (= C-H stretching vibration, sp^2), 2925 (C-H stretching vibration, sp^3), 1708 (C = O ester), 1604 (C = O ketone), 1494 (C = C, Ar), 1519 (Ar-NO_2) para, 1216 (C-O, ester), 831 (C–N). ^{1}H-NMR (400 MHz, DMSO-d_6): δ (ppm) 0.825 (s.3Ha), 1.022 (s.3Ha'), 1.98 (d, J = 16.0 Hz, 1Hb), 2.20 (d, J = 16.0 Hz, 1Hb'), 2.31 (d, J = 16.0 Hz, 1Hc), 2.33 (s, 3Hd), 2.42 (d, J = 16.0 Hz, 1Hc'), 3.53 (s,3Hc), 4.99 (s,

1Hf), 7.41 (d, J = 2.0 Hz, 1Hh), 8.10 (d, J = 12.0 Hz, 2Hg), 9.28 (s, 1Hi). ^{13}C-NMR (400 MHz, DMSO-d_6) δ (ppm) 18.8, 26.9, 29.5, 32.6, 36.9, 39.3, 40.6, 50.5, 102.5, 109.5, 123.7, 129.0, 146.1, 146.9, 150.6, 155.3, 167.3, 194.7.

(1 m): Methyl 4-(3-bromophenyl)-2,7,7-trimethyl-5-oxo-1,4,6,6,8,8-hexahydroquinoline-3-carboxylate [29]. M. P.: 234–236 °C; IR (KBr, cm^{-1}): 3276 (NH stretching), 3077 (=C–H stretching vibration, sp^2), 2958 (C-H stretching vibration, sp^3), 1700 (C = O ester), 1648 (C = O ketone), 1494 (C = C, Ar), 1216 (C–O, ester), 536 (Ar–Br) *meta*.

Conclusion

In this investigation, a facile method for the successful synthesis of a low cost magnetic catalyst is reported by immobilization of Mn(II) on Fe_3O_4@Schiff base. The as-synthesized catalyst shows a good magnetic property, so it can be extracted from the reaction mixture easily and applies in the next catalytic cycles. This catalyst was applied for the synthesis of Hantzsch hydroquinoline derivatives in solvent-free condition with excellent yield in mild reaction condition. Short reaction time, little catalyst loading, easy separation, nano size of the catalyst and high surface to volume ratio are other advantages of this catalytic system.

Acknowledgements We thank the Ahvaz University Research Council (Islamic Azad University) for their support.

Funding There is no funding to report.

Data availability All data generated or analysed during this study are included in this published article.

Code availability Not applicable.

Declarations

Conflict of interest The authors declare that they have no conflict of interest.

References

1. Klusa V (1995) Cerebrocrast. Neuroprotectant, cognition enhancer. Drugs Future 20:135–138
2. Nasr-Esfahani M, Hoseini SJ, Montazerozohori M, Mehrabi R, Nasrabadi H (2014) Magnetic Fe_3O_4 nanoparticles: efficient and recoverable nanocatalyst for the synthesis of polyhydroquinolines and Hantzsch 1,4-dihydropyridines under solvent-free conditions. J Mol Catal A Chem 382:99–105
3. Pastan I, Gottesman M (1987) Multiple-drug resistance in human cancer. N Engl J Med 316:1388–1393
4. Love B, Snader KM (1965) The Hantzsch reaction. I. Oxidative dealkylation of certain dihydropyridines. J Org Chem 30:1914–1916
5. Zhang XY, Li YZ, Fan XS, Qu GR, Hu XY, Wang JJ (2006) Multicomponent reaction in ionic liquid: a novel and green synthesis of 1,4-dihydropyridine derivatives. Chin Chem Lett 17:150–152
6. Mekheimer RA, Hameed AA, Sadek KU (2008) Solar thermochemical reactions: four-component synthesis of polyhydroquinoline derivatives induced by solar thermal energy. Green Chem 10:592–593

7. Das B, Ravikanth B, Ramu R, Rao VB (2006) An efficient one-pot synthesis of polyhydroquinolines at room temperature using HY-zeolite. Chem Pharm Bull 54:1044–1045
8. Reddy CS, Raghu M (2008) Cerium(IV) ammonium nitrate catalysed facile and efficient synthesis of polyhydroquinoline derivatives through Hantzsch multicomponent condensation. Chin Chem Lett 19:775–779
9. Sapkal SB, Shelke KF, Shingate BB, Shingare M (2009) Nickel nanoparticle-catalyzed facile and efficient one-pot synthesis of polyhydroquinoline derivatives via Hantzsch condensation under solvent-free conditions. Tetrahedron Lett 50:1754–1756
10. Li M, Zuo Z, Wen L, Wang S (2008) Microwave-assisted combinatorial synthesis of hexasubstituted 1,4-dihydropyridines scaffolds using one-pot two-step multicomponent reaction followed by a S-alkylation. J Comb Chem 10:436–441
11. Tu SJ, Zhou JF, Deng X, Cai PJ, Wang H, Feng JC (2001) One step synthesis of 4-arylpolyhydroquinoline derivatives using microwave irradiation. Chin J Org Chem 21:313–316
12. Zhu QL, Xu Q (2016) Immobilization of ultrafine metal nanoparticles to high-surface-area materials and their catalytic applications. Chem 1:220–245
13. Hoseini SJ, Nasrabadi H, Azizi M, Salimi Beni A, Khalifeh R (2013) Fe_3O_4 nanoparticles as an efficient and magnetically recoverable catalyst for Friedel-Crafts acylation reaction in solvent-free conditions. Synth Commun 43:1683–1691
14. Sun S, Zeng H (2002) Size-controlled synthesis of magnetite nanoparticles. J Am Chem Soc 124:8204–8205
15. Hoseini SJ, Heidari V, Nasrabadi H (2015) Magnetic Pd/Fe_3O_4/reduced-graphene oxide nanohybrid as an efficient and recoverable catalyst for Suzuki–Miyaura coupling reaction in water. J Mol Catal A Chem 396:90–95
16. Hoseini SJ, Aramesh N, Bahrami M (2017) Effect of addition of iron on morphology and catalytic activity of PdCu nanoalloy thin film as catalyst in Sonogashira coupling reaction. Appl Organomet Chem 31:e3675–e3683
17. Sreedhar B, Kumar AS, Reddy PS (2010) Magnetically separable Fe_3O_4 nanoparticles: an efficient catalyst for the synthesis of propargylamines. Tetrahedron Lett 51:1891–1895
18. Roopan SM, Nawaz-Khan FR, Mandal BK (2010) Fe nano particles mediated C–N bond-forming reaction: regioselective synthesis of 3-[(2-chloroquinolin-3-yl)methyl]pyrimidin-4(3*H*)ones. Tetrahedron Lett 51:2309–2311
19. Lü HY, Yang SH, Deng J, Zhang ZH (2010) Magnetic Fe_3O_4 nanoparticles as new, efficient, and reusable catalysts for the synthesis of quinoxalines in water. Aust J Chem 63:1290–1296
20. Söderlind P, Moore KT (2008) When magnetism can stabilize the crystal structure of metals. Scr Mater 59:1259–1262
21. Nasrabadi H, Amirghofran Z, Esmaeilbeig A, Bahrami M, Hoseini SJ (2018) Covalent bonding of magnetic Fe_3O_4 nanoparticles to aminopropyl-functionalized magnesium phyllosilicate clay: synthesis and cytotoxic potential investigation. Appl Organomet Chem 32:e4036–e4044
22. Tian R, Seitz O, Li M, Hu W, Chabal YJ, Gao J (2010) Infrared characterization of interfacial Si–O bond formation on silanized flat SiO_2/Si surfaces. Langmuir 26:4563–4566
23. Jaleh B, Khalilipour A, Habibi S, Niyaifar M, Nasrollahzadeh M (2017) Synthesis, characterization, magnetic and catalytic properties of graphene oxide/Fe_3O_4. J Mater Sci Mater Electron 28:4974–4983
24. Munasir N, Setianingsih N, Yanasin S, Supardi ZAI, Taufiq A, Sunaryono S (2019) Phase and magnetic properties of Fe_3O_4/SiO_2 natural materials-based using polyethylene glycol media. IOP Conf Ser Mater Sci Eng 515:012017
25. Baran T, Sargın I, Kaya M, Mulercikas P, Kazlauskaite S, Mentes A (2018) Production of magnetically recoverable, thermally stable, bio-based catalyst: remarkable turnover frequency and reusability in Suzuki coupling reaction. Chem Eng J 331:102–113
26. Baran T, Baran NY, Mentes A (2019) Highly active and recyclable heterogeneous palladium catalyst derived from guar gum for fabrication of biaryl compounds. Int J Biol Macromol 132:1147–1154
27. Mirzaee H, Izadyar A, Davoodnia A, Eshghi H (2014) One-pot synthesis of polyhydroquinoline derivatives via Hantzsch condensation reaction using nanosized magnesium oxide as heterogeneous catalyst. J Appl Chem Res 8:57–63
28. Mayurachayakul P, Pluempanupat W, Srisuwannaket C, Chantarasriwong O (2017) Four-component synthesis of polyhydroquinolines under catalyst- and solvent-free conventional heating conditions: mechanistic studies. RSC Adv 7:56764–56770

29. Nagarapu L, Apuri S, Gaddam S, Bantu R, Mahankhali VC, Kantevari S (2008) A facile synthesis of polyhydroquinoline derivatives via the Hantzsch reaction under solvent free-conditions using potassium dodecatungsto cobaltate trihydrate ($K_5CoW_{12}O_{40.3}H_2O$). Lett Org Chem 5:60–64
30. Khazaei A, Zolfigol MA, Moosavi-Zare AR, Afsar J, Zare A, Khakyzadeh V, Beyzavi MH (2013) Synthesis of hexahydroquinolines using the new ionic liquid sulfonic acid functionalized pyridinium chloride as a catalyst. Chin J Catal 34:1936–1944
31. Nagarapu L, Kumari MD, Kumari NV, Kantevari S (2007) MCM-41 catalyzed rapid and efficient one-pot synthesis of polyhydroquinolines via the Hantzsch reaction under solvent-free conditions. Catal Commun 8:1871–1875